Expanded substrate screenings of human and *Drosophila* type 10 17β-hydroxysteroid dehydrogenases (HSDs) reveal multiple specificities in bile acid and steroid hormone metabolism: characterization of multifunctional 3α/7α/7β/17β/20β/21-HSD

Naeem SHAFQAT*, Hanns-Ulrich MARSCHALL†, Charlotta FILLING*, Erik NORDLING‡, Xiao-Qiu WU*, Lars BJÖRK‡, Johan THYBERG§, Eva MÅRTENSSON*, Samina SALIM*, Hans JÖRNVALL* and Udo OPPERMANN*

*Department of Medical Biochemistry and Biophysics, Karolinska Institutet, SE-171 77 Stockholm, Sweden, †Department of Medicine, Karolinska Institutet, Huddinge University Hospital, SE-141 86 Stockholm, Sweden, ‡Biovitrum AB, SE-112 87 Stockholm, Sweden, and §Department of Cell and Molecular Biology, Karolinska Institutet, SE-171 77 Stockholm, Sweden

17β-Hydroxysteroid dehydrogenases (17β-HSDs) catalyse the conversion of 17β-OH (-hydroxy)/17-oxo groups of steroids, and are essential in mammalian hormone physiology. At present, eleven 17β-HSD isoforms have been defined in mammals, with different tissue-expression and substrate-conversion patterns. We analysed 17β-HSD type 10 (17β-HSD10) from humans and *Drosophila*, the latter known to be essential in development. In addition to the known hydroxyacyl-CoA dehydrogenase, and 3α-OH and 17β-OH activities with sex steroids, we here demonstrate novel activities of 17β-HSD10. Both species variants oxidize the 20β-OH and 21-OH groups in C_{21} steroids, and act as 7β-OH dehydrogenases of ursodeoxycholic or isoursodeoxycholic acid (also known as 7β-hydroxylithocholic acid or 7β-hydroxyisolithocholic acid respectively). Additionally, the human orthologue oxidizes the 7α-OH of chenodeoxycholic acid (5β-cholanic acid, 3α,7α-diol) and cholic acid (5β-cholanic acid). These novel substrate specificities are explained by homology models based on the orthologous rat crystal structure, showing a wide hydrophobic cleft, capable of accommodating steroids in different orientations. These properties suggest that the human enzyme is involved in glucocorticoid and gestagen catabolism, and participates in bile acid isomerization. Confocal microscopy and electron microscopy studies reveal that the human form is localized to mitochondria, whereas *Drosophila* 17β-HSD10 shows a cytosolic localization pattern, possibly due to an N-terminal sequence difference that in human 17β-HSD10 constitutes a mitochondrial targeting signal, extending into the Rossmann-fold motif.

Key words: bile acid, *Drosophila*, 17β-hydroxysteroid dehydrogenase (17β-HSD), insect metabolism, short-chain dehydrogenases/reductases, steroid hormone metabolism.

INTRODUCTION

Hydroxysteroid dehydrogenases (HSDs) catalyse the oxidation/reduction of hydroxy (-OH)/oxo groups of steroids. This reaction type not only contributes fundamental steps in the biosynthesis of vertebrate steroid hormones or bile acids, but also has a critical role in maintaining intracellular levels of receptor ligands through tissue-specific expressions of distinct HSDs [1,2]. The enzymes have been grouped according to the reactions carried out at the steroid position [1,2]. Several HSDs show a broad spectrum of enzymic activities towards steroids and other compounds, such as prostaglandins, retinoids and fatty acid derivatives. This complex specificity pattern makes a coherent assignment system difficult.

Mammalian 17β-HSDs form a large family of HSDs, are critically involved in sex steroid metabolism, and consequently control hormone levels of oestrogens and androgens [3]. Most of the vertebrate HSDs characterized to date belong to the conserved protein families of short-chain dehydrogenases/reductases (SDRs) or to aldo–keto reductases (AKRs) [4–7]. The two families differ fundamentally in structure and stereospecificity of hydride transfer, but display a similar chemical mechanism with a conserved tyrosine residue as a catalytic base. At present, 11 distinct forms of 17β-HSDs have been described in mammals, differing in substrate specificities, tissue, developmental and subcellular distribution patterns, and the preferred reaction direction *in vivo*. They all belong, except for 17β-HSD5, to the SDR family.

Type 10 17β-HSD (17β-HSD10) is a mitochondrial enzyme with a substrate specificity encompassing the 17β-OH dehydrogenation of oestrogens, the 3α-OH dehydrogenation of androgens and the oxidation of hydroxyacyl-CoA of fatty acids and branched-chain amino acids [8–11]. It shows a broad expression pattern, with high levels in the liver, brain and gonads [12]. It was initially described as an endoplasmic-reticulum-derived amyloid β-peptide-binding protein (termed ERAB); however, a mitochondrial localization was determined subsequently [12,13]. The importance of this enzyme was demonstrated in studies linking the enzymic activity with increased levels of reactive oxygen species, leading to implications for a role in neurodegenerative disorders such as Alzheimer's disease, or showing elevated expression in the azoospermic w/w^v mouse model [12,14,15]. At present, none of these biological effects potentially mediated by 17β-HSD10 have been resolved to identify conclusively which enzymic activity is responsible. Furthermore, a lethal

Abbreviations used: (CD)CA, (chenodeoxy)cholic acid; ERAB, endoplasmic-reticulum-derived amyloid β-peptide-binding protein; GFP, green fluorescent protein; GC, gas chromatography; 17β/3α/20β/21/7α/7β-HSD, 17β/3α/20β/21/7α/7β-hydroxysteroid dehydrogenase; 17β-HSD10, type 10 17β-HSD; IMAC, immobilized metal-ion-affinity chromatography; (iso)UDCA, (iso)ursodeoxycholic acid; -OH, -hydroxy; SDR, short-chain dehydrogenase/reductase; TMS, trimethylsilyl.

[1] To whom correspondence should be addressed (e-mail Udo.Oppermann@mbb.ki.se).

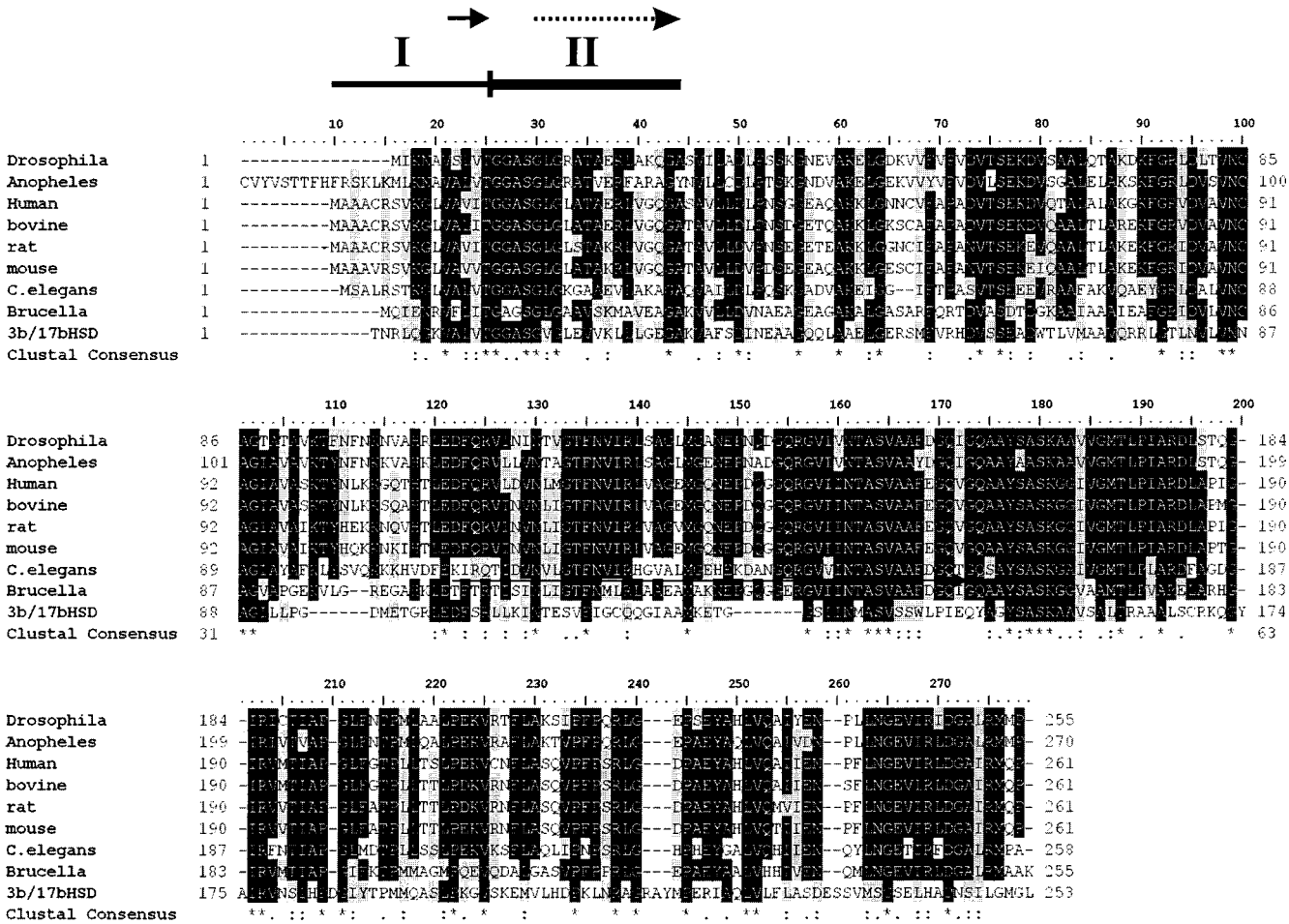

Figure 1 Sequence alignment of 17β-HSD10 orthologues (human, bovine, rat, mouse, *Drosophila melanogaster*, *Anopheles*, *Caenorhabditis elegans*, *Brucella suis*) and a related bacterial HSD (3β/17β-HSD from *C. testosteroni*)

Highly conserved sequence elements of the primary structures are highlighted by black and grey shading. The N-terminal segments (I and II) exchanged in this study between human 17β-HSD10 and bacterial 3β/17β-HSD from *C. testosteroni* are marked. The arrows indicate secondary-structure elements within the targeting sequence, the solid arrow depicts strand βA, and the dotted arrow shows helix αB. The Figure was created using ClustalW and BioEdit packages.

Drosophila mutant has been described with mutations in the *scully* gene [16], which shows approx. 70 % identity with the mammalian 17β-HSD10 enzyme at the amino acid level (Figure 1). However, an enzymological analysis of this enzyme has not been performed. We have therefore now determined a catalytic profile by screening for steroid-metabolizing activities, and compared mammalian and insect forms for functional relationships.

EXPERIMENTAL

Cloning, protein expression and purification

Expression constructs were obtained by cloning human and *Drosophila* 17β-HSD10 into pET15b vectors (Novagen) by PCR using cDNA libraries from human liver and *Drosophila* (Stratagene). The expression plasmids code for N-terminal His_6-tagged proteins containing an internal thrombin-cleavage site. Entire construct sequences were verified by analysis on an ABI 377 system. The expression plasmids were transformed into *Escherichia coli* BL21DE3 cells, grown at 37 °C, and recombinant proteins were expressed by isopropyl β-D-thiogalactoside induction at an attenuance of $D_{600} = 0.6$ for 2 h. Cells were harvested, lysed by sonication, and recombinant proteins were purified by IMAC (immobilized metal-ion-affinity chromatography) on His-bind resin (Novagen). Thrombin protease (Amersham Pharmacia Biotech) was used to cleave the His_6-tag. Purity was confirmed by SDS/PAGE, and protein concentrations were determined spectrophotometrically or by compositional analysis on a Biochrome amino acid analyser after hydrolysis of samples in 6 M HCl/0.1 % (v/v) phenol. Assessment of protein conformations was achieved by CD spectroscopy by recording the ellipticity as a function of wavelength between 260 and 195 nm using an AVIV Model62 DS spectropolarimeter.

Drosophila 17β-HSD10 was subcloned from the pET construct into the pEGFP-N3 vector (Clontech). Human 17β-HSD10 was amplified by PCR from a human liver cDNA library and cloned into the Bluescript^{KS} vector (Stratagene) using specific primers and *Eco*RI/*Bam*HI restriction sites (Table 1). These constructs were used for further subcloning. GFP (green fluorescent protein) constructs were obtained using the pEGFP-N3 vector. Sequences around the initiation codon were mutated to conform to Kozak sequence requirements. As a template for 3β/17β-HSD, constructs with the expression vector pET15b (Novagen) were used [17]. Cloning of constructs coding for hybrid proteins (3β/17β-HSD10

Table 1 Oligonucleotide sequences used for construction of human 17β-HSD10 (ERAB) and 3β/17β-HSD hybrid proteins

wt, wild-type.

Name	Sequence	Restriction site	Vector
ERABwt-3′	5′-CTCATGCCGGATCCTCAAGGCTGCATACGAATGGC-3′	*Bam*HI	KS
3βwt-3′	5′-CTAGGGATCCCTATAGCCCCATGCCCAGAAT-3′	*Bam*HI	KS
ERAB-5′	5′-TTGATATCGAATTCACCATGGCAGCAGCGTGTCGGAGC-3′	*Eco*RI	KS
3β-5′	5′-TTGATATCGAATTCAAAATGACAAATCGTTTGCAGGGT-3′	*Eco*RI	KS; pEGFP-N3
ERAB/3β-5′	5′-CTTGATATCGAATTCACCATGGCAGCAGCGTGTCGGAGCGTGAAGGGCCTGGTGGCGGTAATAACTGGTGGTGCCAGCGGTGTGGGT-3′	*Eco*RI	KS; pEGFP-N3
3β/ERAB-5′	5′-CTTGATATCGAATTCAAAATGACAAATCGTTTGCAGGGTAAGGTGGCGCTGGTCACCGGAGGAGCCTCGGGCCTGGGC-3′	*Eco*RI	KS; pEGFP-N3
ERABGFP-5′	5′-ATGCTAGAAAGCTTACCATGGCAGCAGCGTGTCGGAGC-3′	*Hind*III	pEGFP-N3
ERABGFP-3′	5′-CACCATGGTGGTACCAGGCTGCATACGAATGGC-3′	Asp^{718}	pEGFP-N3
3βGFP-3′	5′-GGTGGCGATGGATCCTAGCCCCATGCCCAGAATCGAGTT-3′	*Bam*HI	pEGFP-N3
ERAB-(1–15)	5′-GTGGTGGTGGGATCCTCCGGTTATTACCGCCACCAG-3′	*Sna*BI	pEGFP-N3
ERAB-(1–34)	5′-GTGGTGGTGGGATCCCTGCCCCACAAGTCGCTCCGCCGT-3′	*Bam*HI	pEGFP-N3

and 17β-HSD10/3β) was performed using specific 5′ and 3′ primers with the hybrid partner DNA as the template in a PCR reaction (Table 1). Deletion constructs [17β-HSD10-(1–15)–GFP and 17β-HSD10-(1–34)–GFP] coding for the predicted mitochondrial targeting sequences (amino acids 1–15 and 1–34 respectively) were obtained by PCR using specific primer sets [17β-HSD10-(1–15) and 17β-HSD10-(1–34)] with integrated *Bam*HI restriction sites, and a complementary primer distal to the *Sna*BI site in the pEGFP-N3 vector sequence (5′-GGA CTT TCC TAC TTG GCA GTA CAT C-3′). Amplified DNA was cloned into the *Sna*BI and *Bam*HI sites of the digested 17β-HSD10–GFP construct. The correct sequences of all constructs were verified by DNA sequence analysis (Applied Biosystems).

Determination of kinetic constants for recombinant human and *Drosophila* 17β-HSD10 enzymes

Enzyme activities were measured as NAD(H)-dependent conversions using 3-hydroxybutyryl-CoA, acetoacetyl-CoA and different steroids (Sigma). Steroids were dissolved in methanol or propan-2-ol, and added to a final concentration of 1 % (v/v). Bile acids were dissolved in 50 mM NaOH. Steroid concentrations used, in many cases, were in the range 0 to 100 μM; when the solubility allowed, the concentration range was larger (0–300 μM). Reactions were performed in 1.0 ml aliquots at 25 °C. Activities were recorded by determination of the change in absorbance at 340 nm, using a molar absorption coefficient for NADH (ε) of 6.22 $mM^{-1} \cdot cm^{-1}$. Experiments were performed at various steroid concentrations with saturating concentrations of cofactor (NAD^+, 1 mM; NADH, 200 μM). No depletion of NADH affecting the rate of reduction at low pH was observed under these conditions. Recordings were measured using a Cary 300Bio instrument. pH profiles were obtained using a set of 100 mM phosphate buffers ranging from pH 5 to 10 (0.2 pH unit increments), and under the conditions employed no change in pH was observed. Kinetic constants were calculated from initial-velocity data by direct curve fitting using non-linear regression analysis (GraphPad software, San Diego, CA, U.S.A.).

GC (gas chromatography)–MS and HPLC

For GC-MS analysis, steroids were converted into volatile methyl ester trimethylsilyl (TMS) ether derivatives, as described previously [18]. Compounds were separated isothermically at 280 °C on a fused-silica capillary column coated with 100 % cross-linked methyl silicone (HP-1; Hewlett–Packard, Wiesbaden, Germany). Steroids were identified by comparisons with authentic compounds and retention indices. For GC-MS, derivatives were automatically injected into 1 μl of hexane at 180 °C in splitless mode. The temperature was taken to 220 °C at 20 °C/min and then to 315 °C at 4 °C/min. GC and GC-MS were performed on Hewlett–Packard HP 6890 ChemStation instruments. Glucocorticoid analyses were performed using a Shimadzu stationary system on C_{18} columns with an eluent of 30 % (v/v) acetonitrile/20 mM ammonium acetate, pH 7.0. Detection was carried out at 240 nm.

Homology modelling of human and *Drosophila* 17β-HSD10

Structural models of human and *Drosophila* type 10 17β-HSD were obtained by homology modelling using the ICM program (version 3; Molsoft LLC, San Diego, CA, U.S.A.) [19–21] with the rat 17β-HSD10 structure (Protein Data Bank code 1E6W) as the template. The human and *Drosophila* primary structures show 88 % and 69 % sequence identities respectively with respect to the rat sequence. The homology modelling involves a transfer of coordinates from the template to the target by inferring distance restraints according to the alignment, followed by a Monte Carlo minimization. Loops are individually modelled to find the lowest-energy conformation in a separate step by Monte Carlo minimizations of each loop, while the rest of the structure is held rigid. The resulting structure is then optimized by another round of Monte Carlo minimization. Docking calculations were performed using the ICM program with a flexible side-chain technique [20]. The position of the steroid was chosen arbitrarily, initial placement of the cofactor was as in the crystal structure, the bond angles of the substrates had full freedom, the peptide backbone was kept rigid, and the side-chain χ angles of the enzyme were free, within 7 Å (1 Å $\equiv$ 0.1 nm) from the substrate. Distance restraints (1.8–2.2 Å) were imposed between Tyr^{168} and the OH/oxo group of the steroid, and between cofactor–hydrogen acceptor and donor sites. Each calculation lasted 500000 steps, and was repeated three times with random starting positions in the active site channel, converging to essentially identical results.

Cell culture

COS-7 cells were grown in DMEM (Dulbecco's modified Eagle's medium) supplemented with 10 % (v/v) FCS (fetal-calf serum), 100 units/ml penicillin, 100 mg/l streptomycin and 2 mM

L-glutamine on chamber slides. Transfection experiments were performed with 200 ng of DNA/15000 cells using the Fugene™ reagent method (Boehringer Mannheim). At 24 to 48 h post-transfection, cells were analysed by fluorescence microscopy. Cells were either fixed and permeabilized with methanol or paraformaldehyde/Triton X–100, or were subjected to incubation with MitoTracker dyes (CmxRos and CM.H2Hrox; Molecular Probes) for vital mitochondrial staining.

Fluorescence microscopy

Co-localization double immunofluorescence analysis was performed with a Leica DMR-RXA microscope (Leica Microsystems) set to restricted focal depth using the iris of the oil-immersion lens and the aperture of the epifluorescence system. The microscope was equipped with a filter set to eliminate overlap of the two signals. A cooled three-chip CCD (charged-coupled device) camera (Hamamatsu Photonics, Japan) was used. Images were captured and processed in a Quantimet 550 Pro Image Workstation (Q550IW, Leica). A three-fold convolution step of the images was performed before fusion by using the arithmetic feature.

Immunoelectron microscopy

Transfected cells were fixed for 2 h with 2 % (v/v) formaldehyde and 0.1 % (v/v) glutaraldehyde in PBS, pH 7.3. After rinsing in PBS, the cells were scraped off the dishes and sedimented by centrifugation [11500 ***g*** (12000 rev./min) for 20 min]. The resulting pellet was cut into small pieces, dehydrated consecutively in ethanol (70, 95 and 100 %), and embedded in LR White. The specimens were first incubated in a mixture of equal parts of ethanol and LR White (1:1, v/v) for 30 min, and then left in pure resin for 12–15 h at 4 °C. After two additional incubations in LR White (30 min each), the specimens were encapsulated into gelatin and placed in a UV-polymerization unit for 12–15 h. Thin sections were cut with diamond knives on an LKB Ultrotome IV and picked up on nickel grids coated with a carbon-stabilized Formvar film. For immunogold staining, the grids were placed for 60 min on droplets of PBS/6 % (w/v) BSA/0.005 % (v/v) Tween 20 to block unspecific binding. They were then transferred to primary antibodies diluted in PBS/6 % BSA/0.005 % Tween 20 and incubated for 3 h in a humid atmosphere. After several rinses with PBS/6 % BSA/0.005 % Tween 20, they were placed on droplets of gold-labelled secondary antibodies diluted in PBS/3 % BSA for 1.5 h, washed with PBS/3 % BSA followed by PBS, post-fixed with 2 % (v/v) glutaraldehyde in PBS for 5 min, rinsed with PBS followed by water, and air-dried. After contrast staining with aqueous uranyl acetate for 30 min and alkaline lead citrate for 30 s, the sections were examined under a Philips CM120TWIN electron microscope at 80 kV.

Immunological reagents

Mouse monoclonal antibodies against Grp75 (mitochondria) were purchased from StressGen Biotechnologies Corp. (Victoria, BC, Canada). Mouse anti-GFP (Clontech) and rabbit anti-Cpn10 (mitochondria; StressGen) were used. TRITC (tetramethylrhodamine β-isothiocyanate)- or FITC-labelled secondary antibodies were from Dako (Stockholm, Sweden). Goat anti-mouse IgG conjugated to 10 nm colloidal gold particles and goat anti-rabbit IgG conjugated to 5 nm colloidal gold particles were purchased from Sigma (Sweden).

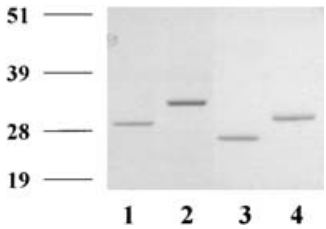

Figure 2 Purification of recombinant 17β-HSD10 from *Drosophila* and human after IMAC

Lanes were loaded as follows: lane 1 and 2, human; lanes 3 and 4, *Drosophila*. Experiments are shown before (lanes 1 and 3) and after (lanes 2 and 4) protease cleavage of affinity tags. The values on the left refer to the masses of molecular markers (in kDa).

RESULTS

Heterologous expression, purification and kinetic analysis of 17β-HSD10 forms

Both 17β-HSD10 species variants were expressed as His_6-tagged fusion proteins in *E. coli* BL21 DE3 cells and purified to apparent homogeneity (Figure 2).

Screening of pH conditions for dehydrogenase and reductase reactions using hydroxybutyryl-CoA and acetoacetyl-CoA as substrates revealed pH optima of 9.3 for the dehydrogenase reaction (for both human and *Drosophila* enzymes) and pH 7.0 (human) and pH 6.4 (*Drosophila*) for the reduction. These results corroborate earlier data obtained with the human enzyme [10], and were employed in all further assays. A steroid substrate screening at saturating cofactor and steroid concentrations was performed (Table 2) using steroids or lipids known to be substrates for the human enzyme. This analysis revealed that both forms catalyse the interconversion of β-OH/oxo groups at position 17 of androgens [testosterone (4-androstene,17β-ol,3-one) and 5α-dihydrotestosterone (5α-androstan-17β-ol,3-one)] and oestrogens, have 3α-HSD activity with androsterone (5α-androstan-3α-ol-17-one), and convert fatty-acyl CoAs (Table 3), largely in line with earlier data obtained for the human enzyme [10]. In our kinetic analysis, we identified approx. 10-fold lower k_{cat}/K_m values with androsterone compared with previous results [9]; however, K_m values were nearly identical, i.e. we believe that the differences observed are either due to distinct reaction parameters or are related to the accuracy of protein determinations, which we performed by compositional analysis after hydrolysis.

Both enzymes catalyse efficiently the NADH-dependent reduction of acetoacetyl-CoA, with similar k_{cat}/K_m values of 55.6×10^6 (human) and 50.2×10^6 (*Drosophila*) $min^{-1} \cdot M^{-1}$, whereas oxidation of 3-hydroxybutyryl CoA showed a markedly higher k_{cat}/K_m value for the human form (3.4×10^6 $min^{-1} \cdot M^{-1}$) compared with 0.67×10^6 $min^{-1} \cdot M^{-1}$ for *Drosophila* (Table 3). 3α-HSD activity with androsterone as substrate showed a markedly higher k_{cat}/K_m value for *Drosophila* when compared with the reported human data (0.33×10^6 $min^{-1} \cdot M^{-1}$ compared with 0.014×10^6 $min^{-1} \cdot M^{-1}$; [9]).

An extended steroid substrate screen was performed, using initially the photometric method, which, in the case of observed absorbance changes, was complemented by product analysis using reversed phase (RP)-HPLC or GC-MS of TMS ethers (Figure 3). Kinetic data were obtained using the photometric method. This approach revealed that both forms catalyse conversions of distinct bile acids or iso-bile acids. Using GC-MS analysis, 3-oxo and 6-oxo product formation was excluded, and therefore not any of 3α-HSD (bile acids), 3β-HSD (iso-bile acids) or 6α-HSD (muricholic acid) activities were present. However, we did detect

Table 2 Comparison of specific steroid activities of human and *Drosophila* 17β-HSD10

Recordings were carried out at substrate and cofactor concentrations (NAD^+ 1.0 mM, NADH 200 μM, steroid 100 μM) at pH 9.3 for dehydrogenase (-DH) and pH 6.4 for reductase (-Red) activities in 100 mM potassium phosphate buffer. na, no activity detected.

			Steroid activity (nmol/mg per min)	
Substrate	Cofactor	Activity type	Human	*Drosophila*
Androsterone	NADH	17oxo-Red	na	na
Dehydroepiandrosterone	NAD^+	3β-DH	na	na
Dehydroepiandrosterone	NADH	17oxo-Red	na	na
Androstenedione	NADH	3/17oxo-Red	na	na
5α-Androstanedione	NADH	3/17oxo-Red	na	na
Adrenosterone	NADH	3/11/17oxo-Red	na	na
5α-Dihydrotestosterone	NAD^+	17β-DH	5 $\pm$ 0.6	2.8 $\pm$ 0.06
5α-Dihydrotestosterone	NADH	3oxo-Red	6 $\pm$ 1.2	21.4 $\pm$ 3
17β-Dihydroandrosterone	NAD^+	3α/17β-DH	52.2 $\pm$ 8.6	96.0 $\pm$ 7
Testosterone	NAD^+	17β-DH	1.1* $\pm$ 0.2	5.7 $\pm$ 1
Testosterone	NADH	3oxo-Red	na	na
Oestradiol	NAD^+	17β-DH	15.6* $\pm$ 0.8	23.7 $\pm$ 4
5α-Pregnan-3β-ol-20-one†	NAD^+	3β-DH	na	na
5α-Pregnan-3β-ol-20-one	NADH	20oxo-Red	na	na
5α-Pregnan-20β-ol-3-one‡	NAD^+	20β-DH	117 $\pm$ 4	78.4 $\pm$ 10
5α-Pregnan-20α-ol-3-one†	NAD^+	20α-DH	na	na
4-Androsten-11β-ol-3,17-dione	NAD^+	11β-DH	na	na
Cortisol§	NAD^+	21-DH	1.9 $\pm$ 0.2	1.7 $\pm$ 0.2
Cortisone§	NAD^+	21-DH	2.3 $\pm$ 0.46	9.6 $\pm$ 0.6
Dehydrocorticosterone§	NAD^+	21-DH	18.2 $\pm$ 0.7	34.2 $\pm$ 2.0
20-Hydroxyecdysone‖	NAD^+	2β/3β/14α/20β/22/25-DH	na	5.8 $\pm$ 0.9
Isoursodeoxycholic acid‡	NAD^+	7β-DH	8.6 $\pm$ 3	8.1 $\pm$ 2
Ursodeoxycholic acid‡	NAD^+	7β-DH	4 $\pm$ 1	4 $\pm$ 0.5
Chenodeoxycholic acid‡	NAD^+	7α-DH	13 $\pm$ 1	na
Cholic acid‡	NAD^+	7α-DH	6.1 $\pm$ 1.2	na
Deoxycholic acid†	NAD^+	3α/12α-DH	na	na
Glycodeoxycholic acid†	NAD^+	3α/12α-DH	na	na
Hyodeoxycholic acid†	NAD^+	3α/6α-DH	na	na
7β-Hydroxycholesterol	NAD^+	3β/7β-DH	na	na

* Values taken from [8].
† Identification/verification via GC.
‡ Identification/verification via GC-MS.
§ Identification/verification via RP-HPLC.
‖ Oxidation of impurities, steroid conversion excluded by electrospray ionization–MS.

Table 3 Kinetic constants for dehydrogenase and reductase activities of 17β-HSD10 from human and *Drosophila*

Values shown are the average of three to five experiments and its corresponding standard deviation value. Measurements for fatty-acyl derivatives are performed at pH optimum (reduction pH 7.0, oxidation pH 9.3) for the human enzyme and for the *Drosophila* enzyme (reduction pH 6.4, oxidation pH 9.3). nd, not determined; na, no activity detected. *Values cited from [8]; †values from [9].

	Kinetic parameter							
Species . . .	Human				*Drosophila*			
Substrate	K_m ($\times 10^{-6}$ M)	k_{cat} (min^{-1})	k_{cat}/K_m (10^6 $min^{-1} \cdot M^{-1}$)	$K_{mNAD(H)}$ ($\times 10^{-6}$ M)	K_m ($\times 10^{-6}$ M)	k_{cat} (min^{-1})	k_{cat}/K_m (10^6 $min^{-1} \cdot M^{-1}$)	$K_{mNAD(H)}$ ($\times 10^{-6}$ M)
Acetoacetyl-CoA/NADH	25.7 $\pm$ 0.9	1430 $\pm$ 70	55.6	30.6	33.7 $\pm$ 8	1660 $\pm$ 187.5	50.2	32.5
β-Hydroxybutyryl-CoA/NAD^+	85.2 $\pm$ 7.2	290.0 $\pm$ 10	3.4	42.3	101 $\pm$ 8	68.0 $\pm$ 5.5	0.67	64.4
Androsterone/NAD^+	45 $\pm$ 9.3*	0.66 $\pm$ 0.08*	0.014*	242*	37.3 $\pm$ 2	12.6 $\pm$ 0.65	0.33	124
Androsterone/NAD^+	41 $\pm$ 14	0.04 $\pm$ 0.005	0.001	nd	–	–	–	–
5α-Dihydrotestosterone/NADH	112 $\pm$ 18†	1.94 $\pm$ 0.21†	0.017†	nd	12.3 $\pm$ 1	4.6 $\pm$ 0.85	0.37	nd
17β-Oestradiol/NAD^+	43 $\pm$ 2.1*	0.66 $\pm$ 0.01*	0.015*	50*	11.1 $\pm$ 2.3	0.52 $\pm$ 0.15	0.048	nd
5α-Pregnan-20β-ol-3-one	5 $\pm$ 1	0.25 $\pm$ 0.035	0.053	nd	9 $\pm$ 2	0.076 $\pm$ 0.01	0.008	nd
Isoursodeoxycholic acid	219 $\pm$ 20	0.054 $\pm$ 0.012	0.0002	nd	3 $\pm$ 0.3	0.014 $\pm$ 0.003	0.005	nd
Chenodeoxycholic acid	36.4 $\pm$ 5.1	0.034 $\pm$ 0.003	0.001	nd	na	–	–	–
Dehydrocorticosterone	1.7 $\pm$ 0.02	0.03 $\pm$ 0.0001	0.018	nd	nd	–	–	–

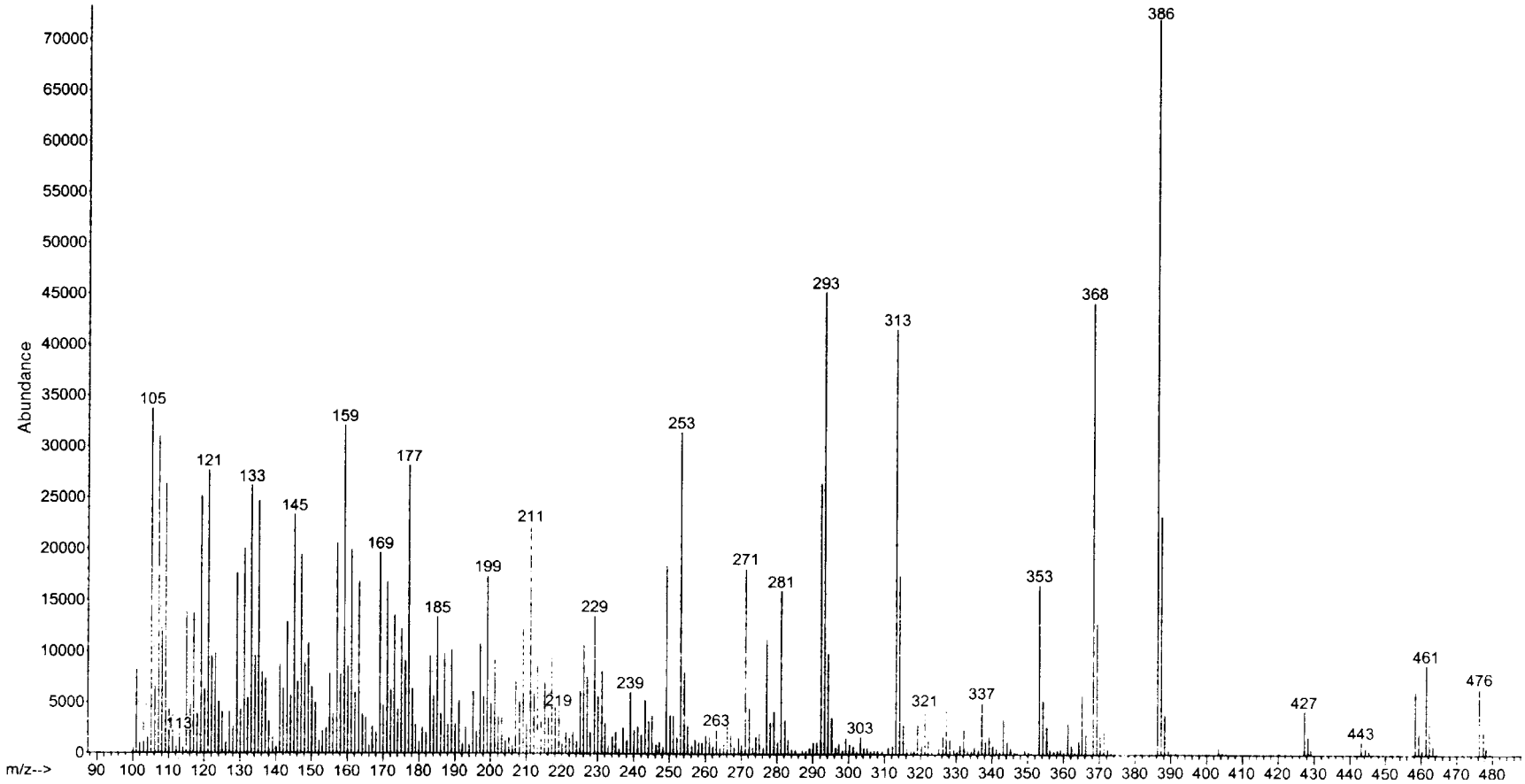

Figure 3 Product formation of steroid conversions determined by GC-MS

A representative example of the mass spectrum and fragmentation pattern of the methyl-ester TMS-ether derivative of 3α-OH,7-oxo-5β cholanoic acid (*m/z* 476 for M^+) is shown.

Table 4 Molecular distances obtained from docking results of human and *Drosophila* 17β-HSD10

Distances between atoms involved in catalysis are given in Å.

Complex	Bond (Å) (molecule)		
	H–O (tyrosine)	O–H (serine)	H–C4 (NAD)
HSD10_hu:isoUDCA	2.2	2.1	2.3
HSD10_Dro:isoUDCA	2.1	2.1	2.1
HSD10_hu:CDCA	2.2	1.8	2.4
HSD10_hu:pregnanolone	1.8	1.8	2.2
HSD10_Dro:pregnanolone	1.7	1.9	2.2
HSD10_hu:cortisol	2.2	2.0	2.2
HSD10_Dro:cortisol	2.1	2.0	2.2

oxidative conversion of the 7α-OH bile acids CA (cholic acid) and CDCA (chenodeoxycholic acid) with human, but not *Drosophila*, 17β-HSD10, whereas both forms converted 7β-OH groups in UDCA (ursodeoxycholic acid; also known as 7β-hydroxylithocholic acid) or iso UDCA (isoursodeoxycholic acid; also known as 7β-hydroxyisolithocholic acid) (Tables 2 and 3, and Figure 3). Furthermore, using GC-MS or HPLC, we detected 20β-OH and 21-OH activities of C_{21} steroids, such as 5α-pregnane,20β-ol,3-one, and glucocorticoids, e.g. cortisol, cortisone or dehydrocorticosterone, respectively. (Table 2). The 20β-OH dehydrogenase shows a k_{cat}/K_m value of 0.053×10^6 $min^{-1} \cdot M^{-1}$ (human) and 0.008 $min^{-1} \cdot M^{-1}$ (*Drosophila*), whereas 21-OH dehydrogenase activity using dehydrocorticosterone as substrate with the human enzyme was found to occur with a k_{cat}/K_m of 0.018×10^6 $min^{-1} \cdot M^{-1}$ (Table 3). The substrate screen included, as a representative for insect steroids, the hormone 20-OH ecdysone (2β,3β,14α,20*R*,22*R*,25-hexahydroxy-5β-cholest-7-ene-6-one); however, the noted absorbance change in the photometric assay (Table 2) was due to substrate impurities when products were analysed by electrospray ionization (ESI)–MS.

Structural evaluation of the active site and substrate docking

Homology modelling of human and *Drosophila* 17β-HSD10 enzymes was performed, using as the template the high-resolution crystal structure of rat 17β-HSD10 ([22]; PDB 1E6W). Inspection of the active sites reveals a large hydrophobic cavity, similar to that described for the rat enzyme [22]. Within this active site, substrate docking with pregnanolone, isoUDCA, CDCA and cortisol as representative substrates was performed, and we obtained atomic distances compatible with enzyme catalysis (Table 4 and Figure 4). Accordingly, the active site of 17β-HSD10 is built up to accommodate the steroid molecule in different orientations in relation to the active-site residues Ser^{155} and Tyr^{168} and the nucleotide cofactor (Figure 4), explaining the multiple steroid specificities observed in our substrate screen. In an earlier study, we demonstrated co-ordination for 17β-OH steroids in the active site, and excluded 3α-OH activities for bile acids [23].

Subcellular localization of human and *Drosophila* 17β-HSD10

Subcellular localization of human and *Drosophila* 17β-HSD10 enzymes was investigated using N-terminal fusion constructs of 17β-HSD10 fused to the GFP reporter. After transfection into COS cells, fluorescence microscopy revealed co-localization with mitochondrial markers for human 17β-HSD10, but not for the *Drosophila* form (results not shown). To analyse the mitochondrial targeting motif in human 17β-HSD10, several hybrid constructs were prepared, transiently expressed and analysed by both fluorescence and electron microscopy studies. A schematic representation of the different constructs is given in Figure 5. The region for mitochondrial targeting was mapped by fusing 17β-HSD10 amino acid residues 1–15 or 1–34, containing secondary structural elements βA-(1–15) to αB-(1–34) of native SDR enzymes (Figures 1 and 5) as N-terminal fusion partners, to GFP (Figure 6, panels A–F). Whereas fluorescence distributed diffusely all over the cell without any indication of mitochondrial targeting is observed in the amino acids 1–15 construct (Figures 6A–6C), a clear punctate-granular staining pattern corresponding to mitochondrial localization is observed in the amino acids 1–34 construct (Figures 6D–6F), thus identifying this sequence region as a mitochondrial targeting signal.

Owing to the high sequence similarities in the 15–34 amino-acid portion of 17β-HSD10 to corresponding regions in SDR enzymes, we reasoned that this segment might be exchangeable with those of other SDR proteins. To test this hypothesis, the N-terminal sequences between human 17β-HSD10 (residues 1–15) and the related enzyme 3β/17β-HSD from *Comamonas testosteroni* (residues 1–12) were exchanged to yield constructs with N-terminal 17β-HSD10 and core 3β/17β-HSD sequences (17β-HSD10–3β-HSD) and vice versa (3β/17β-HSD–HSD10) (Figures 1, 5, 7G–7L and Table 1). These constructs were used for mitochondrial-import analysis when fused to GFP as a reporter molecule. Fluorescence microscopy analysis revealed that 17β-HSD10–3β-HSD indeed is retained substantially within mitochondrial structures (Figure 6, panels J–L). In contrast, the fluorescence of the 3β/17β-HSD–HSD10 construct is distributed over the cytoplasmic compartment without any notable mitochondrial enrichment (Figure 6, panels G–I), reflecting the data obtained with the wild-type 3βHSD–GFP construct (cytoplasmic location; results not shown). Electron microscopy of the same sets of experiments confirmed these observations. First, the localization to mitochondria is detected in 17β-HSD10–GFP-transfected cells. Second, using the N-terminal shuffled targeting constructs, primary localization of 17β-HSD10–3β-HSD constructs to mitochondria, and loss of this organelle localization with the 3β/17β-HSD–HSD10 construct, was observed. Thus 17β-HSD10 and 17β-HSD10–3β-HSD are translocated into mitochondria, whereas 3β-HSD and 3β/17β-HSD–HSD10 are not (Figure 7), confirming the data from the fluorescence microscopy experiments. Taken together, these results indicate that the sequence of the first 34 amino acid residues of the 17β-HSD10 protein is sufficient to direct and translocate 17β-HSD10 to mitochondria, and therefore constitutes a mitochondrial targeting sequence. Furthermore, the data indicate that the targeting sequence is composed of at least two different segments. Segment 1 includes the amino acids 1–15, comprising the β-strand βA (inferred from SDR crystal structures), and is specific for 17β-HSD10. Segment 2 comprises the amino acid sequence 15–34 and α-helix αB, and can be replaced with a corresponding conserved segment from other SDR enzymes, such as prokaryotic 3β/17β-HSD (Figures 1, 5, 6 and 7).

DISCUSSION

Enzymic properties and functions of 17β-HSD10

The physiological role of 17β-HSD10 is at present poorly understood. We therefore analysed functional properties of the human and *Drosophila* orthologues using a wide range of different steroid substrates. Unexpectedly, we found several novel activities of 17β-HSD10, with specificities both on axial and equatorial

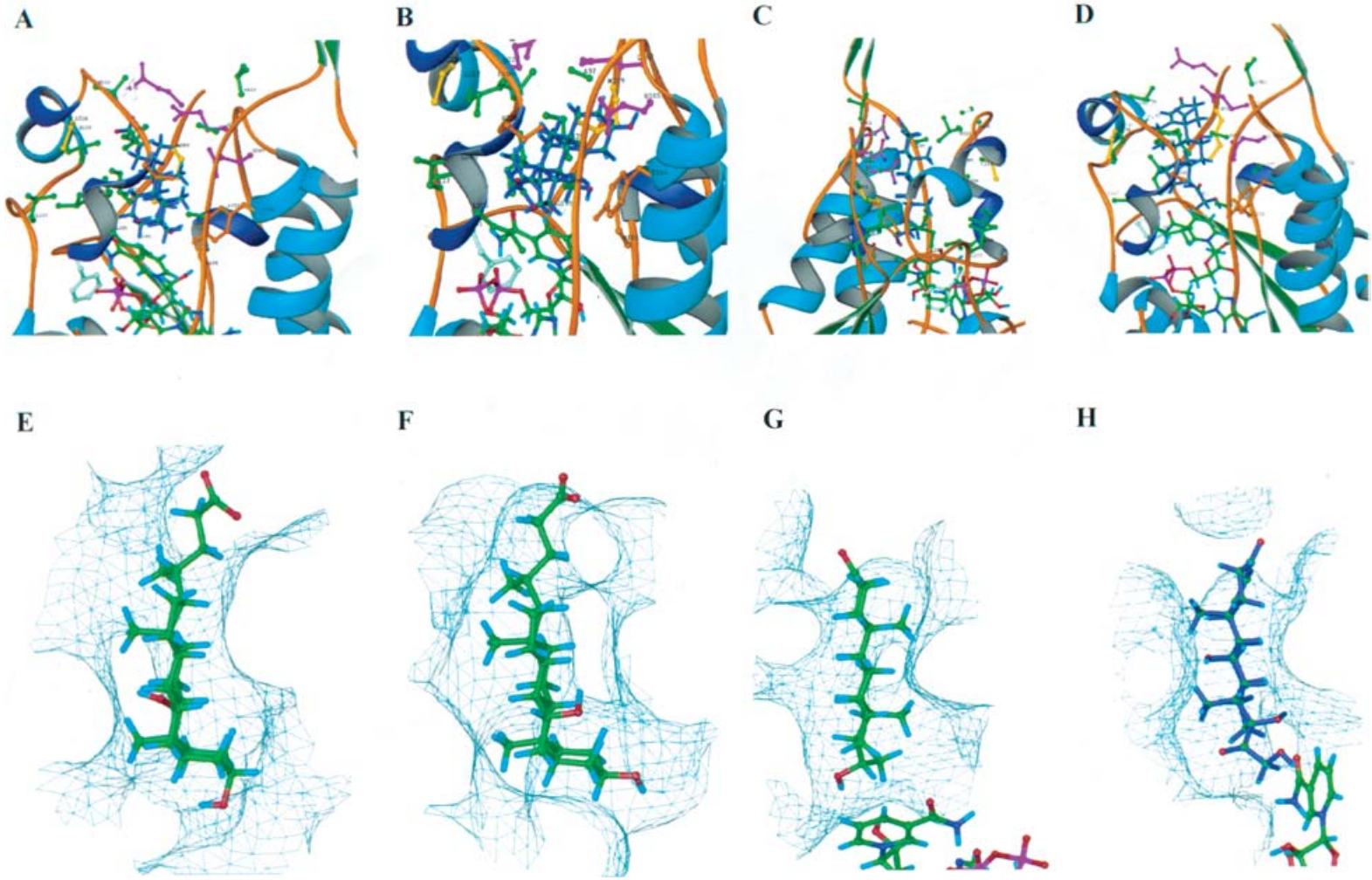

Figure 4 Binding modes for substrates in the active site of human 17β-HSD10 in relation to residues necessary for catalysis and the coenzyme molecule

The structure was obtained using rat 17β-HSD10 as template, performed with the program ICM. Catalytic residues (Ser^{138} and Tyr^{151}; side-chains shown in orange) (**A**–**D**) and residues forming van der Waals contact with the substrates are shown. The complementarity between the different substrate molecules and parts of the accessible surface area of human 17β-HSD10 (**E**–**H**) is also shown. (**A** and **E**) 7β-HSD configuration, substrate isoUDCA; (**B** and **F**) 7α-HSD configuration, substrate CDCA; (**C** and **G**) 20β-HSD, substrate 5α-pregnane,20β-ol,3-one. (**D** and **H**) 21-HSD configuration, substrate cortisol. The Figure was created with RIBBONS.

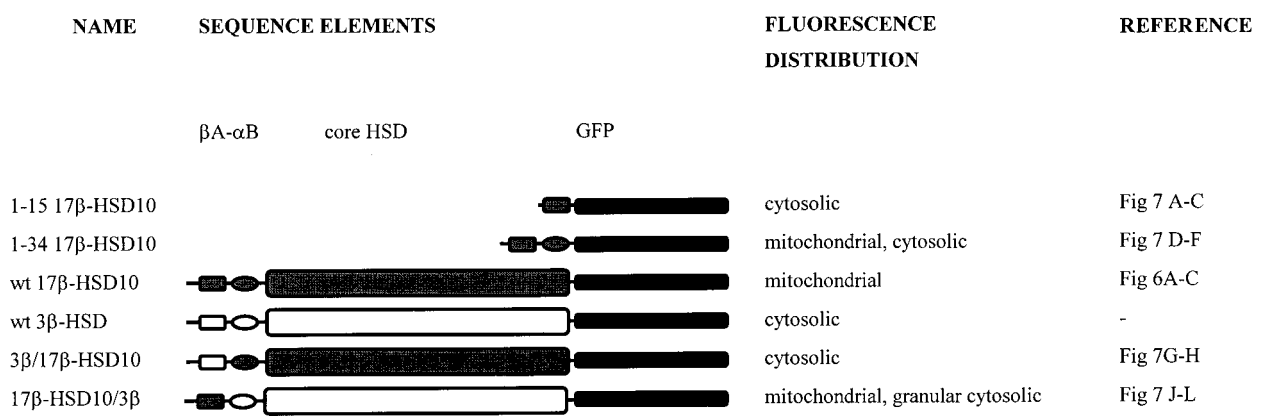

Figure 5 Graphical representation and subcellular distribution of wild-type, deletion and hybrid GFP constructs with human 17β-HSD10 used in this study

Secondary structure elements βA and αB are depicted as rectangles and ellipses, respectively, with the core SDR protein displayed as larger rectangles (17β-HSD10 in grey, 3β-HSD in white). These constructs were fused to the GFP passenger protein (displayed as the black rectangle). Subcellular distribution and specific mitochondrial localization, determined by fluorescence microscopy as well as references to Figures 6 and 7 for the respective constructs, are indicated.

positions of the steroid molecule, which could be explained by docking and modelling experiments based on an orthologous high-resolution structure (of the rat enzyme). These results establish 17β-HSD10 as a remarkably 'promiscuous' dehydrogenase, with a wide substrate spectrum. The obtained k_{cat} values are markedly lower for steroid conversions as compared with fatty acid derivatives, but the steroid data obtained for 17β-HSD10 in the present study are comparable with that of other HSDs with a proven *in vivo* relevance [1–3,5]. However, evaluation of the role *in vivo* requires further experimentation.

As determined in this study, 17β-HSD10 carries out oxidative conversions of 7-hydroxylated bile acids. In humans, normal bile contains glycine- or taurine-conjugated primary bile acids (CDCA and CA), secondary bile acids (LCA and DCA, formed by bacterial 7α-dehydroxylation from CDCA and CA respectively during the enterohepatic circulation) and UDCA. UDCA is believed to be formed concertedly from CDCA in the intestine by bacterial C7-epimerization, i.e. 7α-dehydrogenation, followed by reduction to the 7β-hydroxylated compound, previously shown to take place also in the liver [24,25]. We therefore characterized a human liver dehydrogenase that is active in oxidizing bile acids with either a 7α- or a 7β-OH group. Thus 7-oxo bile acids such as 7-oxo-CDCA may be formed in the liver, and serve as a source for UDCA. Recent data obtained from primary human hepatocytes indicate that the liver does indeed produce UDCA from CDCA (M. Axelsson and E. Ellis, personal communication), supporting the suggested epimerization pathway of 7α-HSD leading to 7-oxo-CDCA, followed by formation of 7β-hydroxylated UDCA by a 7-oxoreductase.

The 20β-OH and 21-OH dehydrogenase activities observed with C_{21} steroids suggest a general role of 17β-HSD10 in controlling the levels of progesterone and glucocorticoid hormone levels. Although several mammalian 20β-HSDs have been identified [1,2,26,27], to our knowledge no identification of 21-HSD has been achieved [28,29]. The 21-HSD activity identified for 17β-HSD10 might therefore be involved with the production of highly polar glucocorticoid C_{21} carbonic acids in conjunction with aldehyde dehydrogenase [30,31].

Sequence comparisons (Figure 1) reveal approx. 70 % identities between mammalian 17β-HSD10 and the protein Scully from *Drosophila*, also suggesting a functional relationship. This is supported by our enzymic data, clearly showing that Scully and mammalian 17β-HSD10 are true orthologues. The *scully* knock-out model [16] shows a lethal phenotype during embryonic and pupal development, affecting germ-line formation, since mutants display non-functional gonads. Expression is found in many insect tissues, including the CNS (central nervous system), and is highest in gonads. Importantly, lipid accumulation and aberrant mitochondria were observed. This localization pattern resembles remarkably closely the situation found with 17β-HSD10 in studied mammalian systems [12,15]. Our enzymic profile shows that Scully (alias *Drosophila* 17β-HSD10) carries out two types of activity, i.e. fatty acid metabolism (third step in β-oxidation) and HSD activities with different specificities on steroids. However, it is at present not possible to decide which of these enzymic functions causes the observed phenotypes in *Drosophila*. Importantly, the role of vertebrate-type steroids and steroid-metabolizing activities (including 17β-HSD, 3α-HSD, 20α-HSD and 20β-HSD), and the β-oxidation pathways in insects, have not been investigated as deeply as in mammalian systems [16,32–35].

Subcellular localization of 17β-HSD10

Whereas human 17β-HSD10 is localized to mitochondria, the *Drosophila* orthologue is not. *Drosophila* 17β-HSD10 has a shorter N-terminal sequence than the human form (Figure 1), which explains the lack of mitochondrial targeting. To understand the targeting events, we investigated the factors governing subcellular localization of human 17β-HSD10 expression, and we established the structural motifs responsible for mitochondrial targeting of human 17β-HSD10. Deduced from the bovine orthologue, the mature 17β-HSD10 protein sequence starts at Ala^2, thus representing a protein with a non-cleavable mitochondrial targeting signal. As determined in our study, the sequence necessary for mitochondrial import involves residues 1–34, characterized by the high content of basic and hydrophobic residues and including the secondary-structure elements βA–αB of the native enzyme. This is in contrast with a previous report [13] showing a mitochondrial targeting signal to reside within the first 15 residues. At present, we cannot explain the observed differences, but our experiments using various experimental parameters (transfection time, plasmid DNA and cell numbers) fail to show mitochondrial targeting with a signal peptide derived from amino acids 1–15. Mitochondrial import of 17β-HSD10 via the 1–34 amino acid motif is likely to involve the well-established route, i.e. after cytosolic synthesis and transport, binding of the targeting

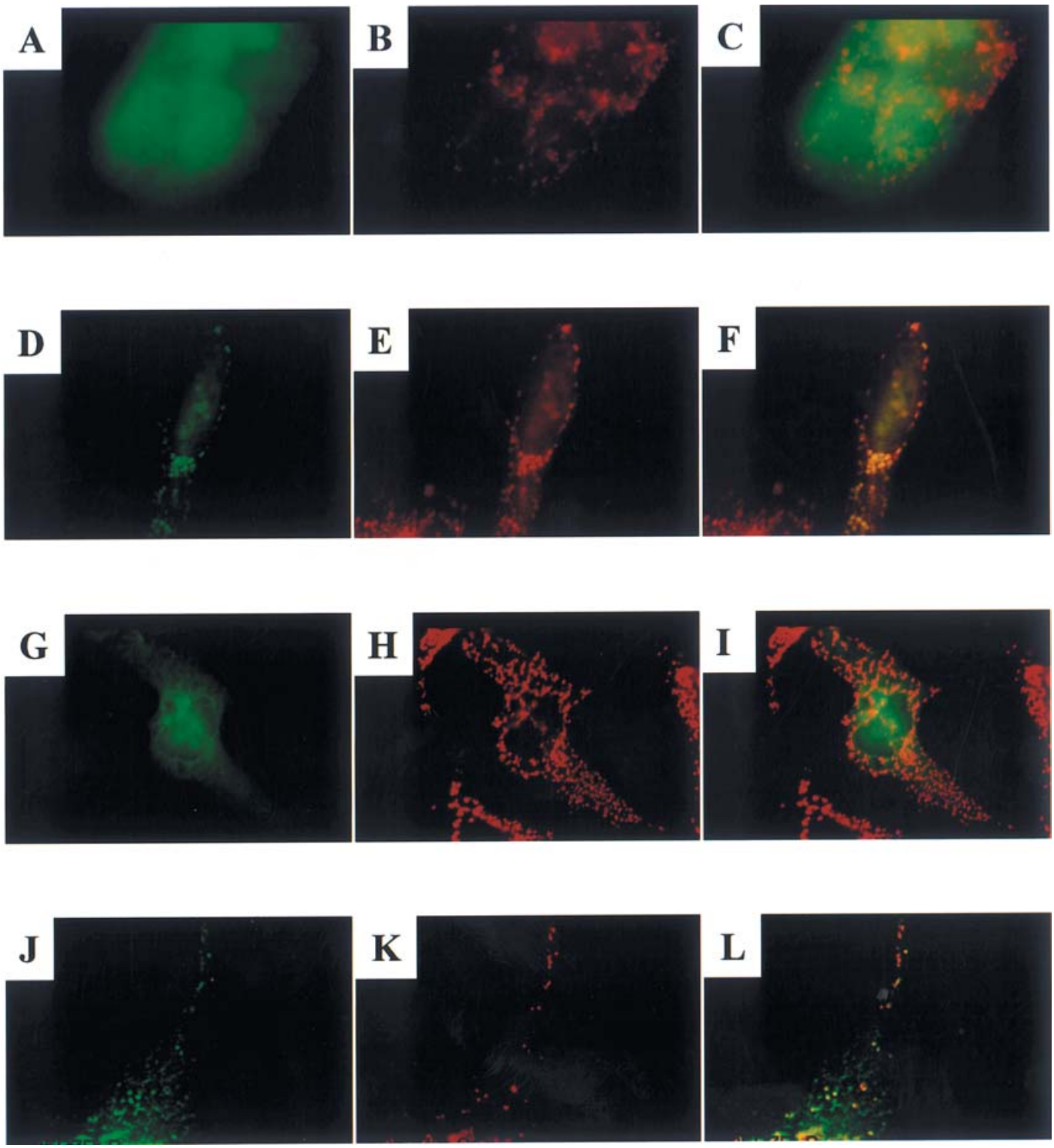

Figure 6 Mitochondrial targeting analysis of human 17β-HSD10-derived peptides fused to GFP

Construct 1–15 (**A**–**C**) and construct 1–34 (**D**–**F**). (**A** and **D**) GFP fluorescence; (**B** and **E**) MitoTracker analysis; (**C** and **F**) overlay of (**A**) + (**B**) and (**D**) + (**E**) respectively. No mitochondrial targeting is observed with the 1–15 construct, whereas mitochondrial co-localization is detected with the 1–34 hybrid. Magnification shown in (**A**)–(**F**) is 1053×. Co-localization of GFP hybrids with exchanged N-terminal motifs is shown: (**G**–**I**) 3β/ERAB hybrids; (**J**–**L**) ERAB/3β hybrids. (**G** and **J**) Fluorescence of hybrid GFP constructs. (**H** and **K**) mitochondrial co-localization using Grp75 antibodies; (**I** and **L**) overlays of (**G**) + (**H**) and (**J**) + (**K**) respectively. No mitochondrial localization is observed with the 3β/ERAB (**G**) construct, whereas some of the ERAB/3β-GFP fluorescence is clearly co-localized to mitochondria (**J**), indicating a weak mitochondrial import signal. (**G**–**I**) magnification 663×; (**J**–**L**) magnification 1347×.

sequence to import receptors occurs on the outer mitochondrial membrane [36,37]. This is followed by translocation of the peptide chain through Tom40, the inner mitochondrial complexes Tim23/Tim17/Tim44 and subsequent folding to the native protein by mitochondrial matrix chaperones. However, the 17β-HSD10 targeting motif involves special features. Notably, a transition

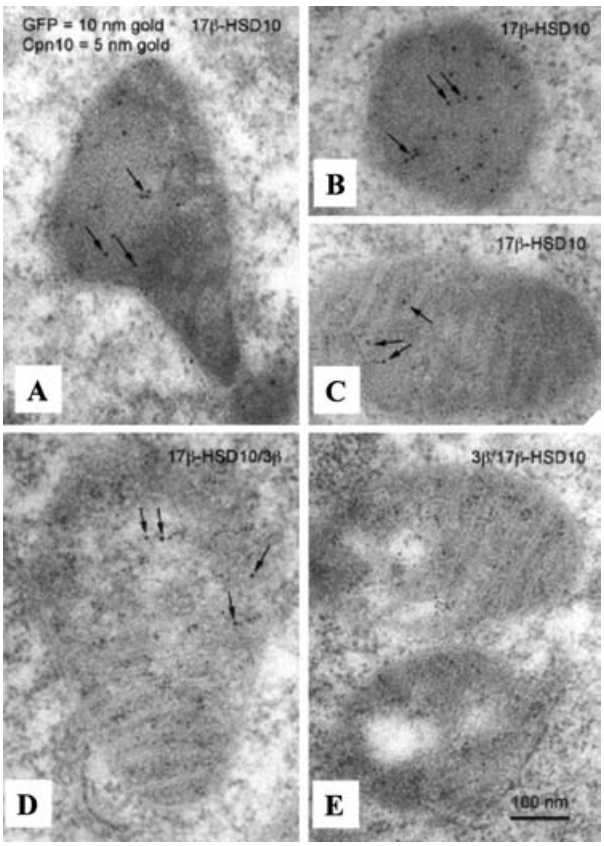

Figure 7 Mitochondrial targeting of different 17β-HSD10 hybrid constructs using immunoelectron microscopy

Expression of different 17β-HSD10 constructs was visualized by using 10 nm gold particles for GFP as hybrid partners to different 17β-HSD10 constructs (shown by arrows), whereas 5 nm gold particles were used to highlight cpn10 as a mitochondrial marker (see the Experimental section). (**A**–**C**) Wild-type human 17β-HSD10. (**A** and **B**) High expression of wild-type 17β-HSD10, showing mitochondrial matrix condensation and partial loss of cristae structure, whereas low or moderate expression of 17β-HSD10 (**C**) reveals a conservation of cristae. (**D**) 17βHSD10/3β construct shows mitochondrial targeting, whereas 3β/17βHSD10 reveals no mitochondrial localization (**E**).

of secondary-structure elements in the N-terminal part of 17β-HSD10 has to occur between the import process and the final matrix-folded state. The 17β-HSD10 targeting motif contains the β-strand βA (cf. Figure 1). which should adopt a helical conformation when interacting with Tom receptors. Thus an amphiphilic helical structure of the targeting peptide allows mitochondrial import in a manner similar to that of other mitochondrial matrix proteins with or without cleavable sequences, e.g. mitochondrial aldehyde dehydrogenase or cpn10. At least, in one example of a non-cleavable matrix-targeted protein, rhodanese, the three-dimensional structures of the synthetic targeting peptide and the holoenzyme have been solved. Differences in secondary structure between the synthetic peptide corresponding to the import sequence (determined by two-dimensional NMR) and the holoenzyme (determined by X-ray crystallography) were then noted, indicating a similar transition as that which we postulate for 17β-HSD10.

Physiological roles of 17β-HSD10

Different functional roles have been suggested for human 17β-HSD10, ranging from involvement in cytotoxic pathways to production of reactive oxygen species [14], linking the binding of amyloid β-peptide with cytotoxicity, activation of androgens (as, for example, 3α-HSD activating androstanediol to 5α-dihydrotestosterone) and the promotion of tumour growth [9]. The phenotype of lipid accumulation in the *Drosophila scully* mutant, lacking 17β-HSD10, prompted us to investigate human patients with proven short-chain hydroxyacyl-CoA dehydrogenase deficiency (C. Filling, B. Keller, D. Hirschberg, E. Kalaitzakis, H.-U. Marschall, H. Jörnvall, M. J. Bennett and U. Oppermann, unpublished work). These data clearly reveal that 17β-HSD10 is not responsible for the phenotypic deficiency by means of its enzymic ability to carry out the 3-hydroxybutyryl-CoA dehydrogenase activity. However, in another recent study on a rare inborn error of metabolism, mutations in the 17β-HSD10/HADH2 gene were found in patients with 2-methyl-3-hydroxybutyryl-CoA dehydrogenase deficiency [11], highlighting the complex multifunctionality of this enzyme in β-oxidation pathophysiology.

We now add several further novel activities to the list that already exists for 17β-HSD10, demonstrating that the enzyme is involved in degradation pathways of glucocorticoids and sex steroids and epimerization of bile acids, besides the oxidation of fatty acids and branched-chain amino acids, thereby constituting a versatile catabolic enzyme. In this manner, 17β-HSD10 represents the oxidative 'counterpart' of another SDR enzyme with a wide substrate spectrum, namely cytosolic NADPH-dependent carbonyl reductase, catalysing the reductive formation of 3α-, 3β- and 17β-OH androstane derivatives, besides prostaglandins and a wide array of xenobiotic substrates [38]. This dichotomy highlights the role of versatile, evolutionarily conserved enzymes mediating catabolic reactions of steroids in mammals and higher eukaryotes, further emphasizing that cytosolic and mitochondrial compartments participate in important biotransformations of lipid mediators and intermediates.

We thank Dr Timo Pikkarainen (of our department) for help with microscopy, and Professor Jan Sjövall (also of our department), Dr Magnus Axelson (Karolinska Hospital) and Dr Ewa Ellis (Huddinge Hospital) for fruitful discussions. The *Drosophila* λ cDNA library was kindly given by R. Gonzalez-Duarte (University of Barcelona, Barcelona, Spain). This study was supported by the European Community (BIO 4 EC 97-2123), the Novo Nordisk Foundation, the Loo och Hans Ostermans foundation, the Swedish Research Council, Karolinska Institutet and BioNetWorks, Germany. S. S. was a recipient of a Wenner-Gren post-doctoral scholarship.

REFERENCES

1 Penning, T. M. (1997) Molecular endocrinology of hydroxysteroid dehydrogenases. Endocr. Rev. **18**, 281–305
2 Nobel, S., Abrahmsen, L. and Oppermann, U. (2001) Metabolic conversion as a pre-receptor control mechanism for lipophilic hormones. Eur. J. Biochem. **268**, 4113–4125
3 Peltoketo, H., Luu-The, V., Simard, J. and Adamski, J. (1999) 17β-hydroxysteroid dehydrogenase (HSD)/17-ketosteroid reductase (KSR) family; nomenclature and main characteristics of the 17HSD/KSR enzymes. J. Mol. Endocrinol. **23**, 1–11
4 Filling, C., Berndt, K. D., Benach, J., Knapp, S., Prozorovski, T., Nordling, E., Ladenstein, R., Jornvall, H. and Oppermann, U. (2002) Critical residues for structure and catalysis in short-chain dehydrogenases/reductases. J. Biol. Chem. **277**, 25677–25684
5 Jez, J. M., Bennett, M. J., Schlegel, B. P., Lewis, M. and Penning, T. M. (1997) Comparative anatomy of the aldo–keto reductase superfamily. Biochem. J. **326**, 625–636
6 Oppermann, U. C., Filling, C. and Jornvall, H. (2001) Forms and functions of human SDR enzymes. Chem. Biol. Interact. **130–132**, 699–705
7 Oppermann, U., Filling, C., Hult, M., Shafqat, N., Wu, X., Lindh, M., Shafqat, J., Nordling, E., Kallberg, Y., Persson, B. and Jornvall, H. (2003) Short-chain dehydrogenases/reductases (SDR): the 2002 update. Chem. Biol. Interact. **143–144**, 247–253
8 He, X. Y., Merz, G., Mehta, P., Schulz, H. and Yang, S. Y. (1999) Human brain short chain L-3-hydroxyacyl coenzyme A dehydrogenase is a single-domain multifunctional enzyme. Characterization of a novel 17β-hydroxysteroid dehydrogenase. J. Biol. Chem. **274**, 15014–15019

9 He, X. Y., Merz, G., Yang, Y. Z., Pullakart, R., Mehta, P., Schulz, H. and Yang, S. Y. (2000) Function of human brain short chain L-3-hydroxyacyl coenzyme A dehydrogenase in androgen metabolism. Biochim. Biophys. Acta **1484**, 267–277

10 He, X. Y., Yang, Y. Z., Schulz, H. and Yang, S. Y. (2000) Intrinsic alcohol dehydrogenase and hydroxysteroid dehydrogenase activities of human mitochondrial short-chain L-3-hydroxyacyl-CoA dehydrogenase. Biochem. J. **345**, 139–143

11 Ofman, R., Ruiter, J. P., Feenstra, M., Duran, M., Poll-The, B. T., Zschocke, J., Ensenauer, R., Lehnert, W., Sass, J. O., Sperl, W. and Wanders, R. J. (2003) 2-methyl-3-hydroxybutyryl-CoA dehydrogenase deficiency is caused by mutations in the HADH2 gene. Am. J. Hum. Genet. **72**, 1300–1307

12 Yan, S. D., Fu, J., Soto, C., Chen, X., Zhu, H., Al-Mohanna, F., Collison, K., Zhu, A., Stern, E., Saido, T. et al. (1997) An intracellular protein that binds amyloid-beta peptide and mediates neurotoxicity in Alzheimer's disease. Nature (London) **389**, 689–695

13 He, X. Y., Merz, G., Yang, Y. Z., Mehta, P., Schulz, H. and Yang, S. Y. (2001) Characterization and localization of human type 10 17β-hydroxysteroid dehydrogenase. Eur. J. Biochem. **268**, 4899–4907

14 Yan, S. D., Shi, Y., Zhu, A., Fu, J., Zhu, H., Zhu, Y., Gibson, L., Stern, E., Collison, K., Al-Mohanna, F. et al. (1999) Role of ERAB/L-3-hydroxyacyl-coenzyme A dehydrogenase type II activity in Aβ-induced cytotoxicity. J. Biol. Chem. **274**, 2145–2156

15 Hansis, C., Jahner, D., Spiess, A. N., Boettcher, K. and Ivell, R. (1998) The gene for the Alzheimer-associated β-amyloid-binding protein (ERAB) is differentially expressed in the testicular Leydig cells of the azoospermic by w/w^v mouse. Eur. J. Biochem. **258**, 53–60

16 Torroja, L., Ortuno-Sahagun, D., Ferrus, A., Hammerle, B. and Barbas, J. A. (1998) *scully*, an essential gene of *Drosophila*, is homologous to mammalian mitochondrial type II L-3-hydroxyacyl-CoA dehydrogenase/amyloid-β peptide-binding protein. J. Cell Biol. **141**, 1009–1017

17 Oppermann, U. C., Filling, C., Berndt, K. D., Persson, B., Benach, J., Ladenstein, R. and Jornvall, H. (1997) Active site directed mutagenesis of 3β/17β-hydroxysteroid dehydrogenase establishes differential effects on short-chain dehydrogenase/reductase reactions. Biochemistry **36**, 34–40

18 Marschall, H. U., Broome, U., Einarsson, C., Alvelius, G., Thomas, H. G. and Matern, S. (2001) Isoursodeoxycholic acid: metabolism and therapeutic effects in primary biliary cirrhosis. J. Lipid Res. **42**, 735–742

19 Cardozo, T., Totrov, M. and Abagyan, R. (1995) Homology modeling by the ICM method. Proteins **23**, 403–414

20 Totrov, M. and Abagyan, R. (1997) Flexible protein-ligand docking by global energy optimization in internal coordinates. Proteins Suppl. **1**, 215–220

21 Abagyan, R., Batalov, S., Cardozo, T., Totrov, M., Webber, J. and Zhou, Y. (1997) Homology modeling with internal coordinate mechanics: deformation zone mapping and improvements of models via conformational search. Proteins Suppl. **1**, 29–37

22 Powell, A. J., Read, J. A., Banfield, M. J., Gunn-Moore, F., Yan, S. D., Lustbader, J., Stern, A. R., Stern, D. M. and Brady, R. L. (2000) Recognition of structurally diverse substrates by type II 3-hydroxyacyl-CoA dehydrogenase (HADH II)/amyloid-β binding alcohol dehydrogenase (ABAD). J. Mol. Biol. **303**, 311–327

23 Nordling, E., Oppermann, U. C., Jornvall, H. and Persson, B. (2001) Human type 10 17 β-hydroxysteroid dehydrogenase: molecular modelling and substrate docking. J. Mol. Graph. Model. **19**, 514–520, 591–593

24 Samuelsson, B. (1959) On the metabolism of ursodeoxycholic acid in the rat. Acta Chem. Scand. **13**, 970–975

25 Gustafsson, B., Norman, A. and Sjovall, J. (1960) Influence of *E. coli* infection on turnover and metabolism of cholic acid in germ-free rats. Arch. Biochem. Biophys. **91**, 93–100

26 Sciotti, M. and Wermuth, B. (2001) Coenzyme specificity of human monomeric carbonyl reductase: contribution of Lys-15, Ala-37 and Arg-38. Chem. Biol. Interact. **130–132**, 871–878

27 Nakajin, S., Takase, N., Ohno, S., Toyoshima, S. and Baker, M. E. (1998) Mutation of tyrosine-194 and lysine-198 in the catalytic site of pig 3α/β, 20β-hydroxysteroid dehydrogenase. Biochem. J. **334**, 553–557

28 Orr, J. C. and Monder, C. (1975) The stereochemistry of enzymic reduction of 21-dehydrocortisol to cortisol. J. Steroid Biochem. **6**, 297–299

29 Lippman, V. and Monder, C. (1978) Purification and properties of an NADPH-dependent 21-oxo-20-hydroxysteroid reductase (17β-aldol reductase) from sheep liver. Isolation of the 20β-glycol product. J. Biol. Chem. **253**, 2126–2131

30 Martin, K. O. and Monder, C. (1978) Oxidation of steroids with the 20β-hydroxy-21-oxo side chain to 20β-hydroxy-21-oic acids by horse liver aldehyde dehydrogenases. J. Steroid Biochem. **9**, 1233–1240

31 Lee, H. J. and Monder, C. (1977) Oxidation of corticosteroids to steroidal carboxylic acids by an enzyme preparation from hamster liver. Biochemistry **16**, 3810–3814

32 Swevers, L., Lambert, J. G. and De Loof, A. (1990) Hydroxysteroid dehydrogenase activity in tissues of two insect species. Comp. Biochem. Physiol. Ser. B **97**, 735–739

33 Swevers, L., Lambert, J. G. and De Loof, A. (1991) Synthesis and metabolism of vertebrate-type steroids by tissues of insects: a critical evaluation. Experientia **47**, 687–698

34 Swevers, L., Lambert, J. G. and De Loof, A. (1991) Metabolism of vertebrate type steroids by tissues of three crustacean species. Comp. Biochem. Physiol. Ser. B **99**, 35–41

35 Webb, T. J., Powls, R. and Rees, H. H. (1995) Enzymes of ecdysteroid transformation and inactivation in the midgut of the cotton leafworm, *Spodoptera littoralis*: properties and developmental profiles. Biochem. J. **312**, 561–568

36 Truscott, K. N., Brandner, K. and Pfanner, N. (2003) Mechanisms of protein import into mitochondria. Curr. Biol. **13**, R326–R337

37 Bauer, M. F., Hofmann, S. and Neupert, W. (2002) Import of mitochondrial proteins. Int. Rev. Neurobiol. **53**, 57–90

38 Wermuth, B. (1995) Expression of human and rat carbonyl reductase in *E. coli*. Comparison of the recombinant enzymes. Adv. Exp. Med. Biol. **372**, 203–209

Received 13 June 2003/30 July 2003; accepted 14 August 2003
Published as BJ Immediate Publication 14 August 2003, DOI 10.1042/BJ20030877